

Predicting New Solids and Superconductors

MARVIN L. COHEN

It is now possible to start with a simple model of a solid composed of atomic cores and itinerant valence electrons and compute the total energy for a given structural arrangement of atoms with enough precision to predict the existence of new solids and their properties. The application of the model based on the pseudopotential method is described with silicon chosen as a prototype material. With only information about the constituent atoms, the electronic, structural, vibrational, and even superconducting properties of solids can be calculated from first principles. The successful predictions of superconductivity in highly condensed hexagonal silicon and the existence of new high-pressure semiconductor phases are highlighted. A discussion is presented of the use of the method to discover new stable or metastable solids at high pressures.

WITH MICROSCOPIC THEORY, IT IS NOW POSSIBLE TO predict the existence and properties of stable solid structures from only the atomic numbers and atomic masses of the constituent elements. Successful examples (1) have led many researchers to believe this is the beginning of an era in which materials with desirable properties will be designed through the use of computers and quantum theory.

Quantum theory was created in the 1920's; but unlike its impact on the study of atoms, its direct application to specific solids was slow in coming. Idealized models of solids were constructed, and the basic physics governing many phenomena such as superconductivity was determined without detailed descriptions of the material-dependent interactions or forces involved. For example, in the highly successful Bardeen-Cooper-Schrieffer (BCS) (2) theory of superconductivity, the nature of the fundamental mechanisms and interactions was determined, but application of the theory to compute such specific properties as the superconducting transition temperatures of particular solids had to wait until a more reliable description of the nonsuperconducting or normal state of the solid was developed.

Why did theoretical understanding of solids lag behind that of atoms? For atoms, the unraveling of optical spectra provided the major insight into their properties. Spectra of gases yield sharp lines that can be interpreted in terms of electron transitions between the discrete energy levels of atoms. When gases become solids, the narrow energy levels of the isolated atoms broaden into bands of energy because of the sharing of electrons between the atoms when they are separated by distances comparable to their sizes. Electron transitions between the widened energy levels in many solids give relatively smooth optical spectra. These spectra bear little resemblance to the sharp lines of the spectra of the constituent atoms and are more difficult to interpret.

Despite their lack of sharp structure, the optical spectra of solids ultimately proved to be rich in information. The use of quantum theory to interpret spectra (3-5) that were modulated (6) to refine their structure resulted in a deeper understanding of the electronic energy bands and of the nature of interactions between particles in solids. By the use of pseudopotentials to determine electronic structure, a realistic, workable model of a solid emerged, a model that is being applied to determine properties of a broad class of condensed-matter systems.

Model of a Solid

Solid-state properties are often dominated by effects that cannot be explained from the properties of isolated atoms. It is the collective and interacting features of a system of atoms that introduce new phenomena. The model used here separates the valence electrons of atoms from their cores, and the solid is viewed as a periodic array of atomic cores or ions embedded in a sea of electrons that were formally the atomic valence electrons (Fig. 1). Each atomic core consists of a positive nucleus surrounded by tightly held core electrons. Once the valence electrons are removed, each core has a positive charge equal to the valence of the atom. It is assumed that the cores are unchanged in the transition from a gas to a solid. Therefore, it is the change in the valence-electron configurations that dictates solid-state properties such as bonding and crystal structure. The result is a simpler quantum mechanical system but still with more than 10^{23} charged particles per cubic centimeter interacting through electromagnetic Coulomb forces.

One approach (1) toward determining crystal structure by this model is to calculate the total energy of a given system for different structural arrangements and separations of the cores. The preferred structure and core separations are then determined under the assumption that the system will have the configuration with the lowest total energy for a specified pressure or volume. Hence, a calculation of the total energy is needed, and it must be precise since the variation in energy with structure can be small. In addition to the kinetic energies of the cores and valence electrons, the total energy includes core-core, electron-core, and electron-electron interactions. The kinetic energies and core-core Coulomb interaction sums are straightforward. The electron-core and electron-electron terms are more formidable, and the success in evaluating the total energy with sufficient precision to obtain structural information depends on the quality of the calculation of these contributions.

Similarly, the evaluation of superconducting properties—such as the transition temperature at which superconductivity occurs—also requires a detailed knowledge of the above interactions plus a description of how the electrons interact with the cores when they are displaced by a lattice vibrational wave.

The author is a professor of physics, University of California, Berkeley, CA 94720, and a faculty senior scientist, Materials and Molecular Research Division, Lawrence Berkeley Laboratory, Berkeley, CA 94720.

The Pseudopotential

A fruitful approach for computing the electron-core and electron-electron interactions is to assume that each electron moves in an average electrostatic potential generated by the cores and other electrons. This one-electron or Hartree model requires a potential $V(\mathbf{r})$ to generate the one-electron wave function $\psi(\mathbf{r})$ by solving Schrödinger's equation

$$\left[\frac{p^2}{2m} + V(\mathbf{r}) \right] \psi(\mathbf{r}) = E\psi(\mathbf{r}) \quad (1)$$

where p , m , and E are the electron momentum, mass, and energy. The electron density $\rho(\mathbf{r})$ at each point in space is given by

$$\rho(\mathbf{r}) = \sum_{\text{electrons}} \psi^*(\mathbf{r})\psi(\mathbf{r}) \quad (2)$$

If both core and valence electrons are considered, the Coulomb potential of the positive nucleus would be used in this all-electron calculation. However, in the pseudopotential model corresponding to Fig. 1, core electron states are not considered. The core potential has a charge equal to the atomic valence ($+4e$ for silicon) at large distance since the negative core electrons balance part of the positive nuclear charge. The core potential is further reduced because the Pauli principle requires that valence electrons be excluded from the core-electron states, and this is manifested as a Pauli repulsive potential that reduces or cancels the Coulomb attraction of the core. A schematic illustration of the cancellation (Fig. 2) shows the reduction of the strong ion potential near the core. The net "pseudopotential" is weaker than the ionic Coulomb potential.

It is customary to use the term "pseudopotential" in connection with models of the type illustrated in Fig. 1 where the core-electron states are not computed or when only the outer part of the valence-electron wave function is studied. In some schemes, such as the empirical pseudopotential method (EPM) (4, 5, 7), experimental data are used as input, while in other ab initio approaches only the atomic numbers of the elements involved are used to generate the pseudopotential.

The pseudopotential method was invented in 1934 by Fermi (8), who used it to compute the perturbation caused by foreign atoms on outer orbits of alkali atoms in a gas. Fermi approximated the valence-electron wave function by a smooth pseudo-wave function without any nodes in the core region. Independently, others (9) recognized the advantages of a pseudopotential approach, and in the late 1950's (10, 11) the Pauli repulsive potential description given here was developed. In the 1960's and 1970's, the EPM was used to (4, 5, 7) unravel optical spectra and electronic structure through the solution of Eq. 1 with experimentally fit Fourier coefficients or form factors of the pseudopotential. Usually only three form factors for

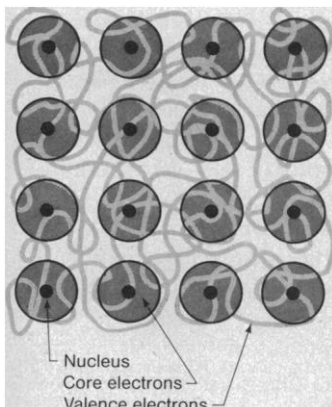
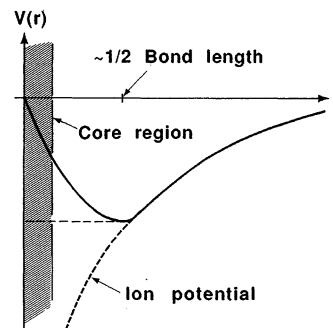


Fig. 1. Pseudopotential model of a solid.

Fig. 2. A schematic pseudopotential showing the reduction of the Coulomb potential near the core.



each element in the solid gave excellent agreement between the calculated properties of a large number of materials and a variety of experimental measurements. The electronic band structures predicted by the EPM are still the most accurate available for many materials.

In the 1970's, technical advances in the pseudopotential method contributed to a renaissance in surface physics. Since electron density readjusts at interfaces, the potential for an electron near an interface can differ considerably from that in the bulk solid. If atoms near the interface are constrained to ideal bulk positions, changes in the electron-electron interactions are responsible for the changes in the potential. Hence, the electron-core and electron-electron potentials need to be treated separately. A powerful approach (12, 13) for surfaces and interfaces is to construct an ab initio pseudopotential for the core and a separate electron-electron potential that depends locally on the density of electrons.

Several similar methods for constructing ab initio pseudopotentials have been developed (1, 14-18). Figure 3 illustrates a pseudo-wave function having no nodes from a standard all-electron 3s radial wave function for silicon. The pseudo-wave function is forced to be identical to the all-electron wave function for distances beyond the outermost maximum where solid-state effects are important. Between the outer maximum and the outermost node, the two wave functions separate, and the pseudo-wave function is smoothly extrapolated to zero with the normalization kept fixed. The generation of a pseudopotential to produce the pseudo-wave function can be illustrated by assuming $\psi(\mathbf{r})$ in Eq. 1 to be a pseudo-wave function and solving for the pseudopotential,

$$V(\mathbf{r}) = E + \frac{(p^2/2m)\psi(\mathbf{r})}{\psi(\mathbf{r})} \quad (3)$$

where p is the operator $-i\hbar\nabla$.

The pseudopotential depends on the orbital angular momentum state of the wave function. Hence, these "nonlocal" pseudopotentials that reflect core-electron differences are constructed for each orbital angular momentum $\ell = 0, 1, 2, 3 \dots (s, p, d, f \dots)$. For example, in silicon there are six core p electrons in the $n = 2$ shell since the atomic core configuration is $1s^2 2s^2 2p^2$, but for carbon, with its $1s^2 2s^2$ configuration, no p electrons exist in the core. Hence, silicon has a strong Pauli repulsive pseudopotential for valence p electrons, whereas carbon has none. Some consequences of this difference will be discussed.

The other important component of the total energy comes from electron-electron interactions. Model potentials have been constructed to simulate the effects of electron-electron Coulomb interactions (Hartree potential), the Pauli principle (exchange potential), and higher-order terms (correlation potentials). The most versatile models are those which depend only on electron density, such as the Thomas-Fermi approximation. A useful approach for calculating ground-state (such as structural) properties of solids is to use a local density approximation (LDA) (19) for the model electron-electron

potentials. In the LDA, each of the above components of the electron-electron potential is expressed in terms of the density $\rho(\mathbf{r})$, and the resulting potential is local, that is, the potential at point \mathbf{r} depends only on the density at \mathbf{r} .

Hence, the "standard" modern pseudopotential approach (1) uses ab initio core pseudopotentials generated from atomic wave functions and the LDA for the electron-electron effects. Another important ingredient in the method is self-consistency. This condition is achieved by solving Eq. 1 for a specific bulk or surface core arrangement with an approximate $V(\mathbf{r})$ to obtain $\psi(\mathbf{r})$ and hence the $\rho(\mathbf{r})$ that is then used to generate the LDA electron-electron potential. The core pseudopotential is added to the LDA potential and Eq. 1 is solved again. When input and output potentials are equal, the calculation is said to be self-consistent. Usually about a half-dozen loops are required.

Structures of Solids

The principal types of crystalline binding (20) are covalent, ionic, metallic, van der Waals, and hydrogen bonding. They originate from electrostatic forces, and, with suitable modifications, the approach described in the previous sections can be applied in all five cases. Pseudopotential applications have focused on the first three types and combinations of them. A triumph of the approach is that the same scheme is used in all cases with comparable success, and no a priori conditions such as a particular choice of wave functions are imposed to comply with specific characteristics of each type of binding. Hence the pseudopotential approach is robust. It can describe the properties of metallic solids with almost constant electron density, or covalent crystals with electronic charge piled up in directional bonds, or ionic compounds in which electronic charge has been transferred between atoms to produce electrostatically interacting charged ions. Only the atomic numbers of the constituent elements that generate the pseudopotentials and a choice of crystal structures are used as input information about the material being examined. The output electron density $\rho(\mathbf{r})$ for the solid displays the bonding nature, and the structural properties are computed directly.

The use of a total energy calculation to search for the lowest energy structure at a given volume has been discussed. Applications have been made to a variety of semiconductors, insulators, and metals. Silicon has been the most-studied material, and its use here illustrates the approach and the results. In Fig. 4, the calculated total energy, at 0 K, is plotted as a function of volume for four possible structures: diamond, white tin, simple (or primitive) hexagonal, and hexagonal close-packed. The volume is normalized to the measured volume in the diamond structure which is both the observed

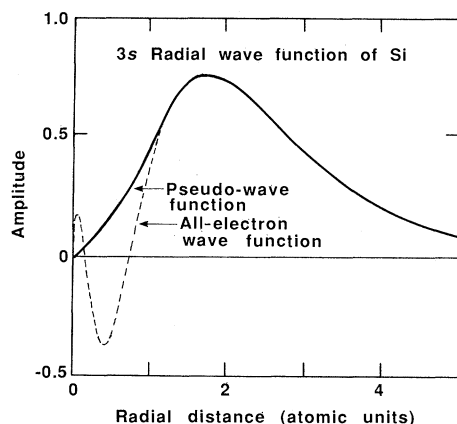
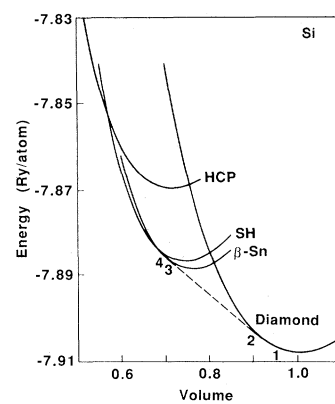


Fig. 3. Comparison of the silicon 3s pseudo-wave function and all-electron wave function.

Fig. 4. Total energy curves for four assumed crystal structures of silicon—diamond, white tin (β -Sn), simple hexagon (SH), and hexagonal close-packed (HCP)—as a function of volume normalized to the zero-pressure volume. The dashed line is the common tangent between the diamond and white-tin structural phases.



atmospheric pressure structure and the lowest energy structure resulting from the calculation. At smaller volumes, which can be achieved with pressure, each of the other structures sequentially becomes lowest in energy (diamond \rightarrow white tin \rightarrow simple hexagonal \rightarrow hexagonal close-packed), and three solid-solid structural phase transitions are possible in this range of volumes.

Table 1. Static structural properties of silicon, germanium, and carbon.

Element	Lattice constant (Å)	Bulk modulus (Mbar)
Silicon		
Calculated	5.45	0.98
Experimental	5.43	0.99
Difference (%)	0.4	-1
Germanium		
Calculated	5.66	0.73
Experimental	5.65	0.77
Difference (%)	0.1	-5
Carbon		
Calculated	3.60	4.33
Experimental	3.57	4.43
Difference (%)	0.8	-2

Several properties of the low-pressure diamond structural phase can be computed from the energy-volume $E(V)$ curve of Fig. 4. The position of the energy minimum gives the volume or lattice constant of silicon. By using the curvature of $E(V)$, the compressibility of silicon or its inverse, the bulk modulus, can be computed. The calculated results for the diamond-structure phases of silicon, germanium, and carbon (Table 1) are in excellent agreement with experimental results. Estimates of the theoretical uncertainties suggest that for many materials agreement on the order of 1% for the lattice constants and 5 to 10% for the bulk moduli is expected.

The structural properties of the high-pressure phases are computed like those of the diamond phase, and the characteristics of the pressure-induced solid-solid phase transitions can be determined. The first high-pressure (low-volume) phase of silicon is the white-tin structural phase (Fig. 4). A common tangent shown by a dashed line is drawn between the diamond and white-tin phases to illustrate the transition path. At the volume corresponding to point 1 in Fig. 4, the system is in the diamond phase. Points 2 and 3 denote the beginning and end of the transition. The volumes at points 2 and 3 are the transition volumes, and these are given by the theory to about 1% of their measured values. At point 4, the entire system is in the white-tin structural phase. Measuring the slope of the dashed line gives the pressure at which the transition occurs. The calculated pressure is 90 kbar, which is within the range of experimental values

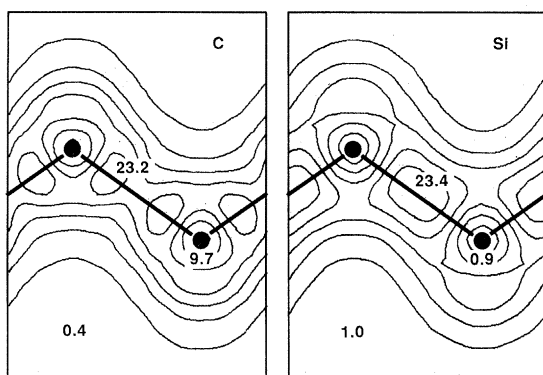


Fig. 5. Total valence charge density plots in the 110 plane for carbon and silicon in the diamond structures. The charge densities are in units of electrons per primitive cell, and the contour step is 4. The axes are scaled to facilitate comparison; hence the length scale is different in these two plots. The black dots denote the atomic positions. Straight lines are drawn to illustrate the atomic chains.

of 88 to 125 kbar. Uncertainties in the calculation suggest that transition pressures for many materials should be calculable within 10% of the experimental value.

The first calculations for silicon predicted a transition to the hexagonal close-packed phase at about 400 kbar. Two experimental groups (21, 22) found this phase at pressures near the predicted value, and in addition discovered the simple hexagonal phase around 130 kbar. When the method was applied to germanium, the transition pressure to the white-tin phase was calculated to be about 100 kbar, which is close to the transition pressure for Si and in agreement with the experiment. However, the transitions to simple hexagonal and hexagonal close-packed were predicted to be much higher in germanium (~800 kbar and >1 Mbar, respectively). The predicted simple hexagonal transition has been verified (23). In contrast, for carbon no transition to simple hexagonal or hexagonal close-packed is predicted (24).

Why do the high-pressure properties of carbon, silicon, and germanium differ? All three are covalent group IV elements with four valence electrons per atom having the s^2p^2 atomic configuration. However, their cores differ, and pseudopotential theory can be used to illustrate the consequences. In Fig. 5, the electronic densities (24) for silicon and carbon are plotted with contour lines of constant density. The plot for carbon shows two peaks along the bond but a single peak for silicon. The origin of this difference is the repulsive p pseudopotential discussed earlier. For silicon the p -core states push the p -valence electrons into the bond to form a single peak. For carbon, there are no p -core states or repulsive p potentials; hence the peak in electron density is near the peak in the density for the atomic p electrons. It is likely that this difference is connected with the multiple bonding character of carbon. Even though carbon and silicon are considered to have similar covalent bonds, the statement "carbon gives biology, but silicon gives geology" (20) and the double-hump versus single-hump charge configuration (Fig. 5) illustrate the difference.

A similar argument relative to d -electron states in the germanium core explains why higher pressures are needed for the transition from white-tin to simple-hexagonal structure but not for that from diamond to white tin. The latter corresponds to s and p properties of the electrons, whereas the former seems to depend on the d nature of the electron states. Both silicon and germanium have p -core electrons, but silicon does not have d states in the core and germanium does. Hence, the repulsive d -potential in germanium keeps valence d states from descending in energy under pressure, and very high pressures are necessary for the structural phase transition.

Superconductivity

A particularly interesting recent development is the application of the methods described here to superconductivity. As described earlier, the BCS theory explains the mechanisms of superconductivity, but a prediction of the transition temperature, T_c , requires precise knowledge of the normal state of the solid. Except for a few cases, theorists have not been successful in predicting new superconductors, nor have they provided significant information on how to raise T_c . Some hints from theoretical studies of the maximum allowed T_c suggest that free electronlike systems are not desirable. Covalentlike charge distributions like those in Fig. 5, but with metallic conduction, seem to be favorable (25) for superconductivity. This observation led to the suggestion that high-pressure metallic simple-hexagonal and hexagonal close-packed silicon would be candidates for superconductivity. The electronic charge densities (26, 27) for these phases are metallic with covalent peaks similar to those shown for silicon in Fig. 5. However, to predict T_c , it is necessary to precisely calculate the interactions that cause superconductivity.

The main interactions determining the superconducting transition are the Coulomb repulsion between electrons and the attractive electron-electron interaction caused by the polarization of the lattice (Fig. 6). The Coulomb repulsion represented by the parameter μ results from the exchange of virtual photons (electromagnetic quanta) between electrons. The attractive term, described by the parameter λ , involves the exchange of phonons which are the quanta associated with lattice vibrations. If $\lambda > \mu$, electrons bind to form pairs; according to the BCS theory (2), the formation of these Cooper pairs is fundamental to the transition to the superconducting state. The BCS transition temperature equation can be written as

$$T_c = E_{ph} e^{-\frac{1}{\lambda - \mu}} \quad (4)$$

where E_{ph} is a phonon energy. Modern versions of Eq. 4 have modified the λ and μ parameters, but the general features are the same.

The pseudopotential approach can be used to compute lattice vibrational frequencies (1) and λ (28) with the atomic mass as the only added input necessary. The calculation of T_c for simple hexagonal silicon is limited by the fact that μ is estimated from previous studies of other superconductors; otherwise the calculation is based on first principles. The predicted T_c is between 5 and 10 K (29), and the calculation indicates that T_c should be a function of pressure. If no structural change takes place in the simple hexagonal phase until the hexagonal close-packed phase is reached at ~400 kbar, the theory predicts that T_c should first decrease with pressure and then rise as the hexagonal close-packed phase is approached. However, a structural transition (21) may occur in this range.

The prediction of superconductivity was confirmed by an experiment (29) in which T_c decreased with pressure up to 260 kbar, the limiting pressure in this first experiment. Although no evidence for a minimum followed by an upturn in T_c (P) appeared in these results, more recent experiments at higher pressures confirmed the theoretical predicted behavior (30).

The Future

The dramatic confirmation of the predictions of new structural phases and superconductivity in simple hexagonal silicon and its pressure dependence give added impetus to this new area. Although silicon was the prototype here, the total-energy-pseudopotential method has been applied to a number of other systems (1). Metals

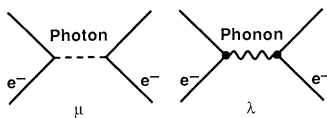


Fig. 6. The dominant electron-electron interactions in superconductors.

from periodic table columns I, II, III, and V have been examined, as have group IV, III-V, II-VI, IV-VI, and I-VII semiconductors and insulators. Measured structural, electronic, vibrational, and structural phase transition properties of these materials have been explained, and, where measurements are not available, theoretical predictions have been made. Some of these predictions have been verified, and others are being examined. Other theoretical approaches (31, 32) have also been successful, particularly with studies of structural properties of metals. Simple *sp* metals, noble metals, transition metals, and even *f*-band metals have been studied.

On the experimental side, the development of diamond anvils, which are constructed from opposed flat diamond surfaces mechanically pushed together, has made high pressures generally available. As a result, theoretical predictions of the properties of solids at high pressures can be tested. Future experimental-theoretical collaborative research will likely test theoretical models, interpret existing data, and predict new materials and properties.

From the point of view of basic science, these studies should clarify the electronic, structural, vibrational, and other properties of matter in transition from atoms to molecules to clusters to extended solids. A knowledge of the properties and interactions will allow theorists to guide experimentalists in their search for new, useful materials. Computer calculations also stimulate the creation of simple models for estimating physical properties. One example of this type of development is that it is now possible to calculate (33) the bulk moduli of a class of semiconductors and insulators on the basis of only the lattice constant of the compound.

It will also be fruitful to search for new metastable phases of solids. For example, a metastable phase of Si exists in the body-centered cubic structure with eight atoms per cell (BC-8), and this phase is calculated to lie above the dotted transition line in Fig. 4. Because the calculated barrier between the white-tin structure and BC-8 is relatively small, it is likely that BC-8 can be produced from the white-tin phase by rapid changes in pressure and temperature. Perhaps other "hidden phases" are accessible in this way. More experience is needed in choosing structures to test, and new approaches are being developed to choose candidate structures using sampling methods such as Monte Carlo techniques.

For superconductivity, the benefits of raising superconducting transition temperatures to high values are enormous. The methods described here suggest that, by studying a variety of systems theoretically, we will be able to isolate the common features of high T_c materials. Studies of the pressure dependences of the various interactions may reveal the origin of the often-noted apparent connection between superconductivity and structural phase transitions.

Theory has moved beyond the highly idealized model stage, and real materials can be examined. These new methods, together with experimental measurements, have helped to clarify some basic properties of solids. In the future, these schemes should lead to the creation of new materials with desirable properties.

REFERENCES AND NOTES

1. M. L. Cohen, *Phys. Scr.* **T1**, 5 (1982).
2. J. Bardeen, L. N. Cooper, J. R. Schrieffer, *Phys. Rev.* **108**, 1175 (1957).
3. J. C. Phillips, *Bonds and Bands in Semiconductors* (Academic Press, New York, 1973).
4. M. L. Cohen and T. K. Bergstresser, *Phys. Rev.* **141**, 789 (1966).
5. J. R. Chelikowsky and M. L. Cohen, *Phys. Rev. B* **14**, 556 (1976).
6. M. Cardona, *Modulation Spectroscopy* (Academic Press, New York, 1969).
7. M. L. Cohen and V. Heine, *Solid State Phys.* **24**, 37 (1970).
8. E. Fermi, *Nuovo Cimento* **11**, 145 (1934).
9. H. Hellmann and W. Kassatotschkin, *Acta Physicochim. URSS* **5**, 23 (1936).
10. J. C. Phillips and L. Kleinman, *Phys. Rev.* **116**, 287 (1959).
11. E. Antonchik, *J. Phys. Chem. Solids* **10**, 314 (1959).
12. M. Schluter, J. R. Chelikowsky, S. G. Louie, M. L. Cohen, *Phys. Rev. B* **12**, 4200 (1975).
13. M. L. Cohen and S. G. Louie, *Annu. Rev. Phys. Chem.* **35**, 537 (1984).
14. T. Starkloff and J. D. Joannopoulos, *Phys. Rev. B* **16**, 5212 (1977).
15. A. Zunger and M. L. Cohen, *ibid.* **18**, 5449 (1978).
16. G. Kerker, *J. Phys. C* **13**, L189 (1980).
17. G. B. Bachelet, D. R. Hamann, M. Schluter, *Phys. Rev. B* **26**, 4199 (1982).
18. S. G. Louie, S. Froyen, M. L. Cohen, *ibid.*, p. 1738.
19. W. Kohn and L. J. Sham, *Phys. Rev.* **140**, A1333 (abstr.) (1965).
20. C. Kittel, *Introduction to Solid State Physics* (Wiley, New York, 1986).
21. H. Olijnyk, S. K. Sikka, W. B. Holzapfel, *Phys. Lett.* **103A**, 137 (1984).
22. J. Z. Hu and I. L. Spain, *Solid State Commun.* **51**, 263 (1984).
23. Y. K. Vohra *et al.*, *Phys. Rev. Lett.* **56**, 1944 (1986).
24. M. T. Yin and M. L. Cohen, *Phys. Rev. B* **24**, 6121 (1981).
25. M. L. Cohen and P. W. Anderson, in *Superconductivity in d- and f-Band Metals*, D. H. Douglass, Ed. (American Institute of Physics, New York, 1972), p. 17.
26. K. J. Chang and M. L. Cohen, *Phys. Rev. B* **30**, 5376 (1984).
27. ———, *ibid.* **31**, 7819 (1985).
28. M. M. Dacorogna, M. L. Cohen, P. K. Lam, *Phys. Rev. Lett.* **55**, 837 (1985).
29. K. J. Chang *et al.*, *ibid.* **54**, 2375 (1985).
30. D. Erskine, P. Yu, K. J. Chang, M. L. Cohen, in preparation.
31. J. A. Moriarty and A. K. McMahan, *Phys. Rev. Lett.* **48**, 809 (1982).
32. V. L. Moruzzi, J. F. Janak, A. R. Williams, *Calculated Electronic Properties of Metals* (Pergamon, New York, 1978).
33. M. L. Cohen, *Phys. Rev. B* **32**, 7988 (1985).
34. Supported by National Science Foundation grant DMR-8319024 and by the director, Office of Energy Research, Office of Basic Energy Sciences, Materials Sciences Division of the Department of Energy under contract DE-AC03-76SF00098.